Atmos. Meas. Tech. Discuss., 7, 8339–8357, 2014
www.atmos-meas-tech-discuss.net/7/8339/2014/
doi:10.5194/amtd-7-8339-2014

Atmospheric Measurement Techniques Discussions
Open Access

Determining the temporal variability in atmospheric temperature profiles measured using radiosondes and assessment of correction factors for different launch schedules

D. Butterfield and T. Gardiner

National Physical Laboratory, Hampton Road, Teddington, Middlesex TW11 0LW, UK

Received: 2 July 2014 – Accepted: 23 July 2014 – Published: 12 August 2014

Correspondence to: D. Butterfield (david.butterfield@npl.co.uk)
and T. Gardiner (tom.gardiner@npl.co.uk)

Published by Copernicus Publications on behalf of the European Geosciences Union.

Determining the temporal variability in atmospheric temperature profiles

D. Butterfield and T. Gardiner

Abstract

Radiosondes provide one of the primary sources of upper atmosphere temperature data for numerical weather prediction, the assessment of long-term trends in atmospheric temperature, the study atmospheric processes and provide a source of intercomparison data for other temperature sensors e.g. satellites. When intercomparing different temperature profiles it is important to include the effect of temporal mis-match between the measurements. To help quantify this uncertainty the atmospheric temperature variation through the day needs to be assessed, so that a correction and uncertainty for time difference can be calculated. Temperature data from an intensive radiosonde campaign were analysed to calculate the hourly rate of change in temperature at different altitudes and provide recommendations and correction factors for different launch schedules. Using these results, three additional longer term data sets were analysed to assess the diurnal variability temperature as a function of altitude, time of day and season of the year. This provides data on the appropriate correction factors to use for a given temporal separation and the uncertainty associated with them. A general observation was that 10 or more repeat measurements would be required to get a standard uncertainty of less than $0.1\,\mathrm{K\,h^{-1}}$ of temporal mis-match.

1 Introduction

Radiosondes provide one of the primary sources of upper atmosphere temperature data and are used globally as input data for numerical weather prediction. Radiosonde data can also be used to assess long-term trends in atmospheric temperature, study atmospheric processes and provide a source of intercomparison data for other temperature sensors e.g. satellites. For many of these applications understanding the measurement uncertainty is crucial to effectively using the data and interpreting the relationship between different measurement sources. The Global Climate Observing System (GCOS) Reference Upper Air Network (GRUAN) has been established under the joint

Discussion Paper | Discussion Paper | Discussion Paper | Discussion Paper |

AMTD

7, 8339–8357, 2014

Determining the temporal variability in atmospheric temperature profiles

D. Butterfield and T. Gardiner

auspices of GCOS and relevant commissions of the World Meteorological Organization (WMO) as an international reference observing network, designed to meet climate requirements and to fill a major void in the current global observing system (Thorne, 2013). Extensive work has been undertaken within GRUAN to establish the traceable measurement uncertainty associated with radiosonde measurements (Immler, 2010). However, when comparing profile results between different atmospheric sensors, the individual sensor measurement uncertainties only make up part of the overall comparison uncertainty. Allowance also has to be made for the co-incidence uncertainty in time and space, and the smoothing uncertainty in the two profile measurements (von Clarmann, 2006). This paper address the co-incidence uncertainty associated with using radiosonde results for intercomparisons with other temperature measurements.

Intercomparisons between temperature measurements made by radiosondes and satellites are well documented (Free, 2005; Randal, 2009). The performance of radiosonde temperature sensors is reasonably well understood and these sensors are normally traceably calibrated on site before launch (Immler, 2010). Whereas satellite sensors are well characterised and calibrated before launch (Mo, 1996), there is no direct mechanism to validate this calibration post-launch or over the time history of the satellite's mission. Drift corrections can be performed (Zou, 2010) and agreements with other satellite measurement methods calculated (Zou, 2014), however these do not make a direct comparison with actual in-atmosphere temperature measurements. Regular intercomparisons between satellite and radiosonde measurements need to be performed to validate the on-going temperature calibration of the satellite. Arranging a coincident satellite overpass of a radiosonde launch is difficult and in most cases impractical. Therefore the rate of change in atmospheric temperature needs to be assessed and an appropriate launch schedule determined to allow valid comparisons. Previous work (Sun, 2010) has found that the mean temperature difference between radiosonde and satellite measurements for a global network to be 0.15 K. The effect of the difference in radiosonde launch time and satellite overpass was also examined.

AMTD
7, 8339–8357, 2014

The comparison standard deviation errors for temperature were found to be 0.35 K per 3 h difference.

This work presents the results of a study of existing radiosonde datasets in order to estimate the uncertainty that would arise due to a temporal mismatch between a radiosonde profile and another source of temperature data. This is derived as a function of altitude, time of day and season of the year. In addition to providing an estimation of the co-incidence uncertainty in time, it also gives guidance on the frequency of radiosonde launches required to capture diurnal variations.

2 Overview and data

To help quantify the difference between radiosonde and satellite measurements the atmospheric temperature variation through the day needs to be assessed, so that a correction for time difference can be calculated. Radiosondes are routinely launched at 12 hourly intervals (00:00 and 12:00 UTC) from many sites around the globe (Seidel, 2006) with a very limited number of sites making more frequent measurements (WMO, 2013). To determine the frequency of launches needed to have an acceptable understanding of the atmosphere's temperature stability over short-time periods (< 24 h), temperature measurements from radiosonde flights at Manus Island, Papua New Guinea, taken during the intensive DYNAMO campaign were analysed. During this campaign, Vaisala RS92-SGP radiosondes with GPS wind finding were launched every 3 h (00:00, 03:00, 06:00, 09:00, 12:00, 15:00, 18:00, 21:00 UTC) from 24 September 2011 to 31 March 2012. After conversion to local time, the hourly rate of change in temperature between launches was calculated for 500 m altitude bins from the surface to 24 km, for launches 3 h, 6 h and 12 h apart. The mean hourly rates of change were inter-compared to assess the launch frequency required to acceptably characterise the diurnal change in temperature.

Following the analysis of launch frequency, long-term data from four radiosonde launches per day at Lindenberg (1999–2008 Vaisala RS90 radiosonde and 2009–

AMTD
7, 8339–8357, 2014

2012 Vaisala RS92-SGP radiosonde) in Southern Germany and Southern Great Plains (Vaisala RS92 radiosonde 2006–2012) Oklahoma, USA were analysed to give hourly rates of change in temperature. Table 1 gives a summary of the radiosonde datasets.

The rate of change data was analysed to show differences in temperature stability between launches over a 24 h period and over the four seasons of the year, again up to an altitude of 24 km. Although some results were available up to 40 km, the number of samples fell off significantly with altitude – as shown in Fig. 1. The maximum altitude of 24 km was selected as a suitable upper limit as all datasets giving > 75 % data capture rates up to this altitude.

3 Results and discussion

3.1 Manus Island DYNAMO data set

From the mean rate of change in temperature between launches 3 h, 6 h and 12 h apart, temperature change profiles over the day were calculated over the range of altitudes and are shown in Fig. 2. The times given in the figure show the mid-point in Local Time (LT) between the two launches used to calculate the temperature differences. Note that, for the 12 h separation results the launch times used are the 00:00 and 12:00 UTC radiosonde launches that are typically used by sites carrying out two launches per day. The error bars on the profiles come from the standard error of the mean. It can be seen in Fig. 2 that the profiles from launches 3 and 6 h apart follow similar profiles during the day, within the error bars (standard error of the mean), while the profiles from launches 12 h apart are unrepresentative and generally underestimate the actual diurnal variability. The profiles shown in Fig. 2 are a subset of all the altitude evaluated. The complete set can be viewed on line in the Supplement.

In order to quantify the difference between the different launch schedules it was assumed that 8 launches per day best described the state of the atmosphere. The mean hourly rates of change in temperature from these launches were therefore considered

AMTD
7, 8339–8357, 2014

to be the base set. The correction factor between the base set and the mean hourly rate of change in temperature for a single launch (i.e. no correction), 2 launches a day and 4 launches a day were calculated, the results of which can be seen in Fig. 3.

It can be seen from Fig. 3 that there is a marked difference in correction factor between 4 launches a day and 2 launches a day, and that there is little improvement in performing 2 launches a day over a single launch. It is therefore assumed in the later analyses that launches spaced 6 h apart provide a reasonable estimation of the hourly rate of change in temperature. Launches spaced 12 h apart do not suitably follow the short-term variations in temperature change over a 24 h period. Clearly this result only directly applies to the Manus dataset, but it provides reasonable confidence in the use of 4 launches per day data for longer term analysis.

3.2 Lindenberg and Southern Great Plains data sets

Once a 6 h launch frequency was accepted to adequately represent the rate of change in temperature, 3 data sets were processed to calculate hourly rates of change between the 4 launches covering a 24 h period. Each data set was broken down into seasons and the calculations repeated to show if there was any changes in behaviour. Subsets of these results are shown in Figs. 4 and 5. Plots for all launches across all seasons can be viewed on line in the Supplement. The error bars represent the standard error of the mean. Note that, as with the Manus data, the launches spaced 12 h apart (at 00:00 and 12:00 UTC) did not show the same degree of diurnal variability as the 6 h launch results.

It can be seen from Fig. 4 that all three datasets show similar behaviour for all launches during winter, except for the Lindenberg 1999–2008 dataset, which shows some divergence in the stratosphere for the rate of change calculated from the 12:00 and 18:00 Local Time launches. Figure 4 shows the results for all four seasons of the rate of change calculated from the 12:00 and 18:00 Local Time launches. In addition to the winter divergence highlighted earlier, the Southern Great Plains (SGP) dataset shows cooling in the stratosphere in spring while the two Lindenberg datasets show heating. SGP shows significantly more heating in the troposphere and above 22 km in the summer. Autumn SGP results are also significantly different from Lindenberg in the lower troposphere, while the two Lindenberg datasets diverge in the stratosphere and are split by the SGP dataset at this altitude. This difference in the stratosphere in the Lindenberg data may be due to the changes in radiosonde type and analysis procedures between the two datasets. The influence of these changes and the effect of improved knowledge of the measurement uncertainty in the more recent data is a potential area for further investigation.

The error bars in Figs. 4 and 5 are expressed as the standard error of the mean result. If the standard deviation for a complete data is calculated and then the standard error calculated for differing numbers of repeat measurements, this gives an indication of the number of repeat measurements/radiosonde flights with corresponding satellite overpasses that would need to be made to bring the uncertainty in the temperature correction into acceptable bounds. Table 2 gives a summary of the mean rate of change in temperature (i.e. the temperature correction factor) between 2 launch times 6 h apart from a single dataset (Lindenberg 1999–2008) along with the standard deviation of the measurements, the standard error of the mean for 10 and 100 repeat measurements for the four seasons of the year. The results for the 3 datasets for all seasons can be viewed on line in the Supplement.

Figure 6 summarises the results at 5 km altitude in Spring to give an indication of the reduction in the uncertainty with increased number of measurements for each dataset. It can be seen that to obtain a standard error of the mean rate of change in temperature of $\leq 0.1\,\mathrm{K\,h^{-1}}$, 10 or more repeat measurements are required. The standard errors of the means for 100 measurements in Table 3 are similar to those for the Manus Island results in Fig. 1 (0.038), which were typically made up of 70 launches per result.

The data in Fig. 6 also shows how these results could be used in practise. Taking the SGP results as an example, if a comparison was made between a single SGP radiosonde temperature measurement and another temperature measurement (between 13:00 and 19:00 Local Time, at 5 km, in Spring) then for each hour difference between

AMTD
7, 8339–8357, 2014

D. Butterfield and T. Gardiner

the measurements a correction of 0.081 K should be applied to the radiosonde result and an additional uncertainty of 0.316 K should be included in the comparison. If this was repeated 10 times the correction factor would remain the same, but the additional uncertainty would reduce to 0.100 K. The overall results presented here enable such an evaluation to be made for any altitude, time of day and season.

4 Conclusions and further work

Four radiosonde datasets have been analysed to assess the temporal variability of the temperature profile as a function of altitude, time of day and season of the year. This provides information on the temporal mis-match uncertainty that would result from comparing atmospheric temperature measurements at different times. The results from the intensive Manus campaign with 8 launches per day show that 2 radiosonde launches per day (at 00:00 and 12:00 UTC) do not capture the diurnal variability and would tend to underestimate both the adjustment and uncertainty that would result from a temporal mismatch, but that 4 radiosonde launches per day provides a reasonable estimate of the diurnal variability.

Analysis of longer term datasets with 4 launches per day provide data on the appropriate correction factors to use for a given temporal separation and the uncertainty associated with them. The uncertainties show similar behaviour for all datasets and indicate that, in general, 10 or more repeat measurements would be required to get a standard uncertainty of less than 0.1 $\mathrm{K\,h^{-1}}$ of temporal mis-match.

It should be recognised that these results only directly apply to the radiosonde launch sites from which the datasets have been obtained. Given the conclusion that at least 4 launches per day are needed to capture the diurnal variability and the very limited number of launch sites from which such long term data is available, then a modification to this analysis would be needed to give it wider global applicability. Two methods to consider are combining twice daily radiosonde results with higher temporal resolution data from another measurement technique or using high resolution meteorological

AMTD
7, 8339–8357, 2014

models to fill in the gaps between the radiosonde launches. Both options will be the subject of further work.

The Supplement related to this article is available online at doi:10.5194/amtd-7-8339-2014-supplement.

Acknowledgements.

Manus

Data provided by NCAR/EOL under sponsorship of the National Science Foundation (http://data.eol.ucar.edu/).

Name: Manus ARM AMF Radiosonde L3 Data (ESC Format) [NCAR/EOL]

URL: http://data.eol.ucar.edu/codiac/dss/id=347.009

This is one of the upper air data sets developed for the Dynamics of the Madden-Julian Oscillation (DYNAMO) 2011–2012 project. This data set includes 1411 high vertical resolution (2 s) soundings from the Atmospheric Radiation Measurement (ARM) C1 Momote. These data were provided by ARM and had preliminarly quality control by NCAR/EOL. This L3 version of the data set has a correction by CSU. This station used Vaisala RS92-SGP radiosondes with GPS wind finding during the DYNAMO field campaign.

Southern Great Plains

Data were obtained from the Atmospheric Radiation Measurement (ARM) Program sponsored by the US Department of Energy, Office of Science, Office of Biological and Environmental Research, Climate and Environmental Sciences Division.

Lindenberg

Data provided by German Meteorological Service (DWD).

The 1999–2009 data is based on radiosonde measurements using Vaisala RS90 instruments.

The 2009–2012 data is a GRUAN data product (RS92-GDP V2) based on radiosonde measurements using Vaisala RS92 instruments. All GRUAN data products are based on measurements and processing that adhere to the GRUAN principles (Immler, 2010). The raw data are

read from the original DigiCora III data base files and are corrected for known systematic biases. The uncertainty of the temperature, the humidity and the wind is calculated from estimates of the calibration uncertainty, the uncertainty of the bias correction and the statistical noise.

References

Free, M. and Seidel, D.: Causes of differing temperature trends in radiosonde upper air data sets, J. Geophys. Res., 110, D07101, doi:10.1029/2004JD005481, 2005.

Immler, F. J., Dykema, J., Gardiner, T., Whiteman, D. N., Thorne, P. W., and Vömel, H.: Reference Quality Upper-Air Measurements: guidance for developing GRUAN data products, Atmos. Meas. Tech., 3, 1217–1231, doi:10.5194/amt-3-1217-2010, 2010.

Mo, T.: Prelaunch calibration of the Advanced Microwave Sounding Unit-A for NOAA-K, IEEE Transactions on microwave theory and techniques, 44, 1460–1469, doi:10.1109/22.536029, 1996.

Randel, W. J., Shine, K. P., Austin, J., Barnett, J., Claud, C., Gillett, N. P., Keckhut, P., Langematz, U., Lin, R., Long, C., Mears, C., Miller, A., Nash, J., Seidel, D. J., Thompson, D. W. J., Wu, F., and Yoden, S.: An update of observed stratospheric temperature trends, J. Geophys. Res., 114, D02107, doi:10.1029/2008JD010421, 2009.

Seidel, D. J. and Free, M.: Measurement requirements for climate monitoring of upper air temperature derived from reanalysis data, J. Climate, 19, 854–871, 2006.

Sun, B., Reale, A., Seidel, D. J., and Hunt, D. C.: Comparing radiosonde and COSMIC atmospheric profile data to quantify differences amoung radiosonde types and the imperfect collocation on comparison statistics, J. Geophys. Res., 115, D23104, doi:10.1029/2010JD014457, 2010.

Thorne, P., Voemel, H., Bodeker, G., Sommer, M., Apituley, A., Berger, F., Bojinski, S., Braathen, G., Calpini, B., Demoz, B., Diamond, H. J., Dykema, J., Fasso, A., Fujiwara, M., Gardiner, T., Hurst, D., Leblanc, T., Madonna, F., Merlone, A., Mikalsen, A., Miller, C. D., Reale, T., Rannat, K., Richter, C., Seidel, D. J., Shiotani, M., Sisterson, D., Tan, D. G. H., Vose, R. S., Voyles, J., Wang, J., Whiteman, D. H., and Williams, S.: GCOS reference upper air network (GRUAN): steps towards assuring future climate records; AIP Conf. Proc., 1552, 1042, doi:10.1063/1.4821421, 2013.

AMTD

7, 8339–8357, 2014

Determining the temporal variability in atmospheric temperature profiles

D. Butterfield and T. Gardiner

Title Page
Abstract Introduction
Conclusions References
Tables Figures
◂ ▸
Back Close
Full Screen / Esc
Printer-friendly Version
Interactive Discussion

von Clarmann, T.: Validation of remotely sensed profiles of atmospheric state variables: strategies and terminology, Atmos. Chem. Phys., 6, 4311–4320, doi:10.5194/acp-6-4311-2006, 2006.

WMO: The GCOS Reference Upper-Air Network (GRUAN) Guide, WIGOS Technical Report No. 2013-03, GCOS-171, 2013.

Zou, C. Z. and Wang, W.: Stability of the MSU derived atmospheric trend, J. Atmos. Ocean. Tech., 27, 1960–1971, doi:10.1175/2009JTECHA1333.1, 2010.

Zou, X., Lin, L., and Weng, F.: Absolute calibration of ATMS upper level temperature sounding channels using GPS RO observations, IEEE T. Geosci. Remote, 52, 1397–1406, doi:10.1109/TGRS.2013.2250981, 2014.

AMTD
7, 8339–8357, 2014

Table 1. Summary of radiosonde datasets used.

Launch site	Manus	Lindenberg	Lindenberg	Southern Great Plains
Latitude	2°3′39.64″ S	52°12′36.0″ N	52°12′36.0″ N	36°36′18.0″ N
Longitude	147°25′31.43″ E	14°7′12.0″ E	14°7′12.0″ E	97°29′6.0″ W
Start	24 Sep 2011	1 Jan 1999	1 Jan 2009	1 Jan 2006
End	31 Mar 2012	31 Dec 2008	31 Dec 2012	31 Dec 2012
Launches per day	8	4	4	4
Sonde	RS92-SGP	RS90	RS92-SGP	RS92-SGP
Total number of launches	1002	14 466	4555	9754

AMTD

7, 8339–8357, 2014

Determining the temporal variability in atmospheric temperature profiles

D. Butterfield and T. Gardiner

Table 2. Lindenberg 1999–2008. Mean rate of change in temperature between launches at 13:00 and 19:00 Local Time at different altitudes for each season, along with standard deviation of a single measurement and standard error with increased number of measurements.

Altitude ~ 5 km	Spring	Summer	Autumn	Winter
Mean rate of change, $\mathrm{K\,h^{-1}}$	0.036	0.040	0.010	0.013
Std Deviation (1 reading)	0.265	0.219	0.304	0.372
Std Error (10 readings)	0.084	0.069	0.096	0.118
St Error (100 readings)	0.026	0.022	0.030	0.037
Altitude ~ 10 km	**Spring**	**Summer**	**Autumn**	**Winter**
Mean rate of change, $\mathrm{K\,h^{-1}}$	0.011	0.027	0.023	0.000
St Deviation (1 reading)	0.305	0.280	0.337	0.368
St Error (10 readings)	0.097	0.088	0.107	0.116
St Error (100 readings)	0.031	0.028	0.034	0.037
Altitude ~ 15 km	**Spring**	**Summer**	**Autumn**	**Winter**
Mean rate of change, $\mathrm{K\,h^{-1}}$	0.006	−0.005	0.004	−0.003
Std Deviation (1 reading)	0.182	0.191	0.215	0.235
Std Error (10 readings)	0.058	0.060	0.068	0.074
Std Error (100 readings)	0.018	0.019	0.021	0.023
Altitude ~ 20 km	**Spring**	**Summer**	**Autumn**	**Winter**
Mean rate of change, $\mathrm{K\,h^{-1}}$	0.031	−0.033	0.032	0.024
Std Deviation (1 reading)	0.199	0.175	0.202	0.270
Std Error (10 readings)	0.063	0.055	0.064	0.085
Std Error (100 readings)	0.020	0.017	0.020	0.027

AMTD
7, 8339–8357, 2014

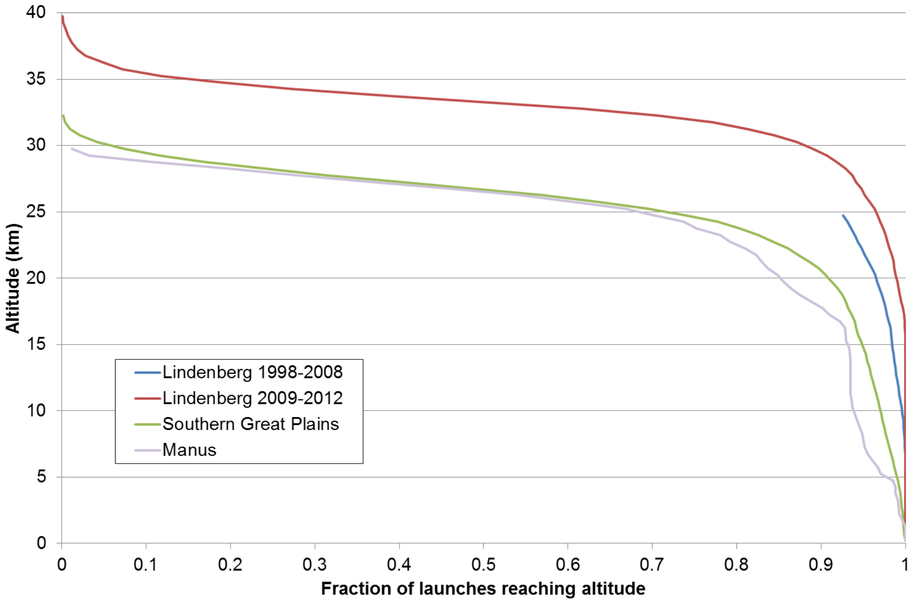

Figure 1. Fraction of radiosonde launches providing results as a function of altitude for each dataset used. Blue line: Lindenberg 1999–2008; red line: Lindenberg 2009–2012; green line: Southern Great Plains; grey line: Manus Island.

AMTD
7, 8339–8357, 2014

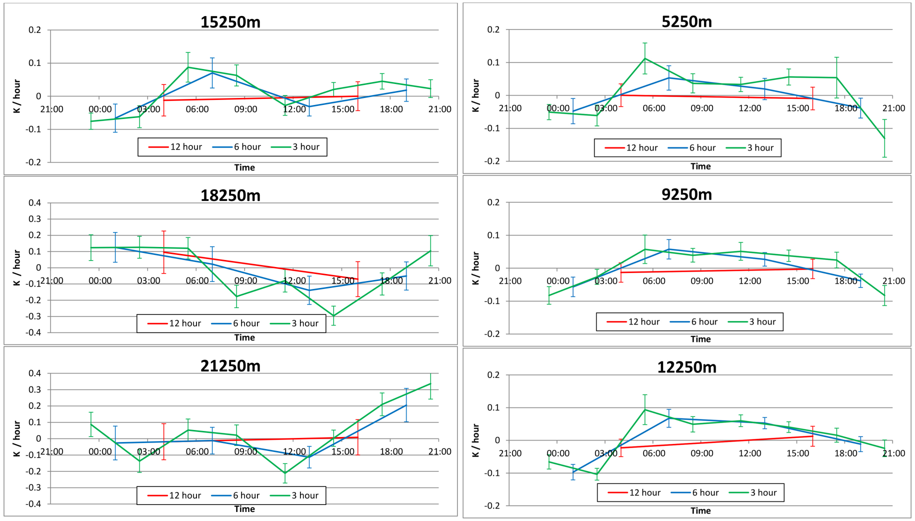

Figure 2. Profiles of mean hourly rate of change in temperature from radiosonde launches from Manus Island during DYNAMO campaign. Error bars are the standard error of the mean. Red line: 12 h separation; blue line: 6 h separation; green line: 3 h separation.

AMTD
7, 8339–8357, 2014

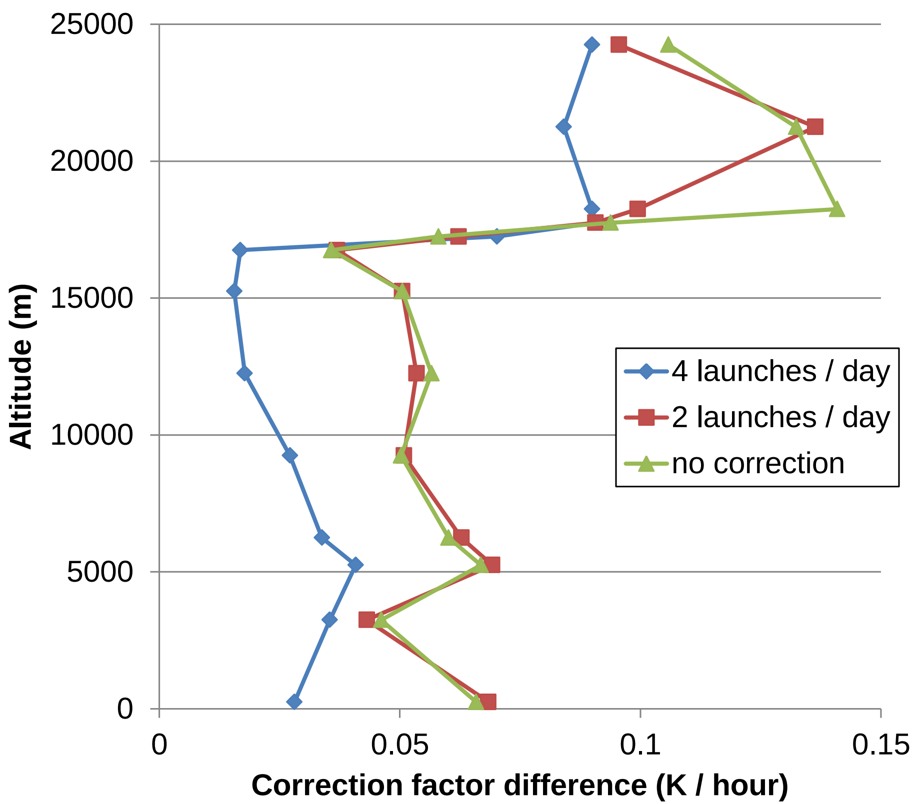

Figure 3. Difference in correction factor for a single launch/no correction (green triangles), 2 launches a day (red squares) and 4 launches a day (blue diamonds).

AMTD
7, 8339–8357, 2014

Determining the temporal variability in atmospheric temperature profiles

D. Butterfield and T. Gardiner

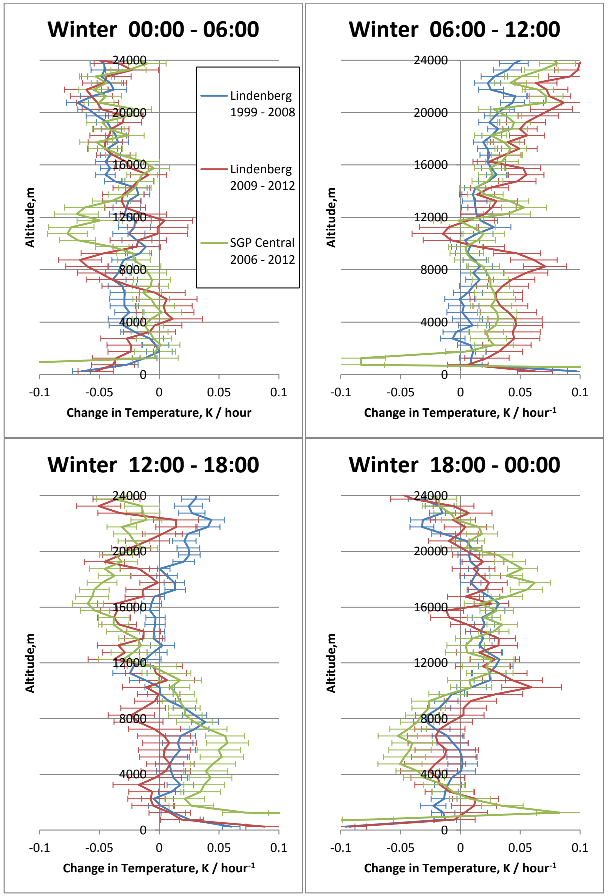

Figure 4. Hourly rate of change in temperature from 0–24 km, for the 3 datasets during winter. Blue line: Lindenberg 1999–2008; red line: Lindenberg 2009–2012; green line: Southern Great Plains.

AMTD
7, 8339–8357, 2014

Determining the temporal variability in atmospheric temperature profiles

D. Butterfield and T. Gardiner

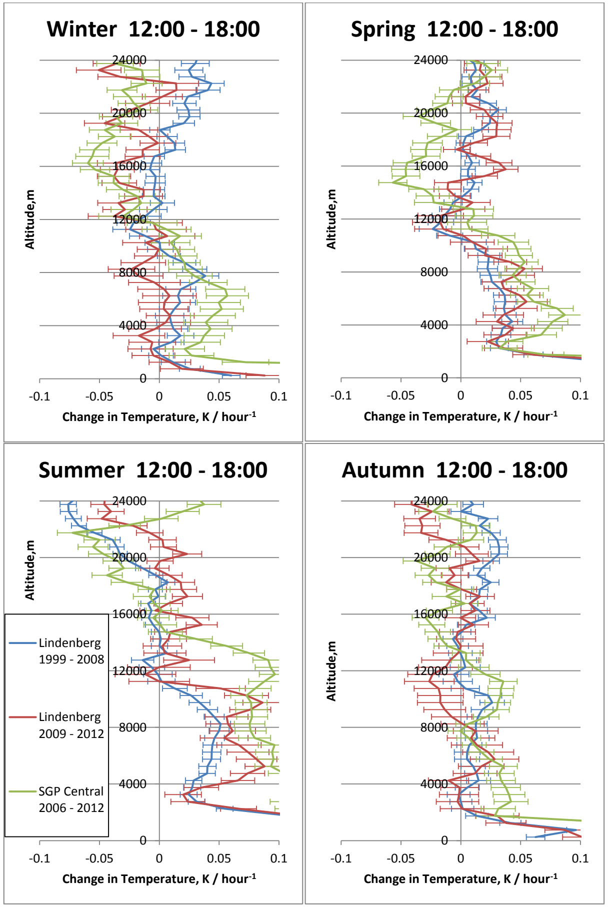

Figure 5. Hourly rate of change in temperature from 0–24 km for 3 datasets, calculated from launches at 12:00 and 18:00 Local Time for all 4 seasons. Blue line: Lindenberg 1999–2008; red line: Lindenberg 2009–2012; green line: Southern Great Plains.

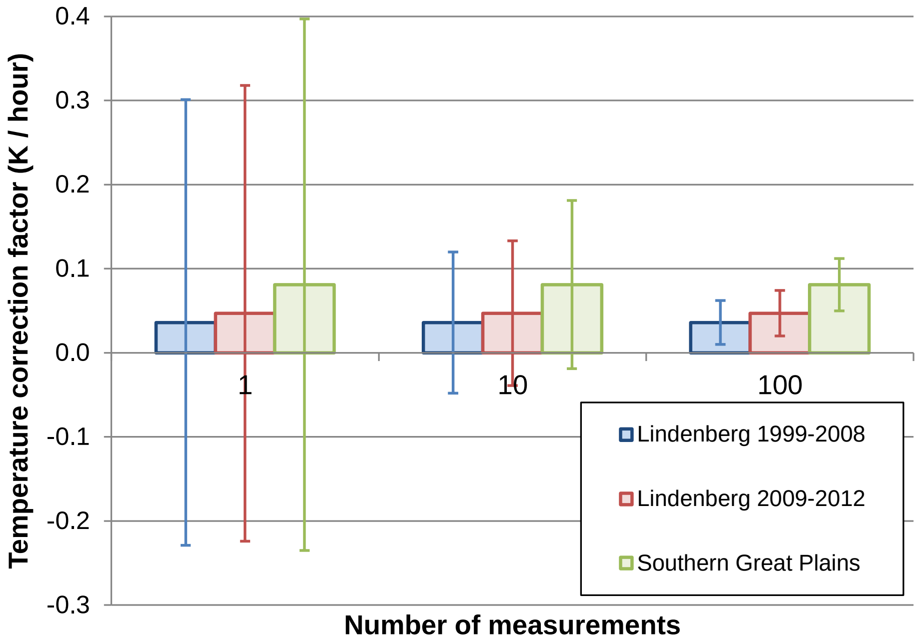

Figure 6. Reduction in uncertainty in hourly rate of change in temperature due to repeat radiosonde flights – for measurements between 13:00 and 19:00 Local Time, at 5 km altitude in Spring. Columns show the mean rate of change of temperature and error bars should the uncertainty associated with different numbers of samples. Blue: Lindenberg 1999–2008; red: Lindenberg 2009–2012; green: Southern Great Plains.

AMTD
7, 8339–8357, 2014

Determining the temporal variability in atmospheric temperature profiles

D. Butterfield and T. Gardiner